



An efficient computational method based on exponential B-splines for a class of fractional sub-diffusion equations

Anshima Singh^{1,*}, Sunil Kumar¹, and Higinio Ramos²

¹Department of Mathematical Sciences, Indian Institute of Technology (BHU) Varanasi, India.

²Scientific Computing Group, Universidad de Salamanca, Plaza de la Merced, Salamanca, 37008, Spain.

Abstract

The primary objective of this research is to develop and analyze a robust computational method based on exponential B-splines for solving fractional sub-diffusion equations. The fractional operator includes the Mittag-Leffler function of one parameter in the form of a kernel that is non-local and non-singular in nature. The current approach is based on an effective finite difference method for discretizing in time, and the exponential B-spline functions for discretizing in space. The proposed scheme is proven to be unconditionally stable and convergent. Also, the unique solvability of the method is established. Numerical simulations conducted for multiple test examples validate the agreement between the obtained theoretical results and the corresponding numerical outcomes.

Keywords. Fractional sub-diffusion equation, Time fractional derivative, Exponential B-spline collocation, Stability analysis, Error bounds.

1991 Mathematics Subject Classification. 65M06, 65M12, 65M70, 35R11.

1. INTRODUCTION

The roots of fractional calculus can be traced back to the 17th century, making its history as ancient and rich as its integer-order counterpart. However, it was during the mid of the last century that the realm of fractional-order differential equations (FODEs) began to flourish. This remarkable development has paved the way for the accurate modeling of numerous phenomena that classical ordinary differential equations (ODEs) struggle to capture. As a result, FODEs have found widespread applications in diverse fields such as chemistry, mathematics, biology, finance, and beyond [1, 2, 40, 44]. The time-fractional subdiffusion equation has diverse applications across scientific and engineering domains due to its ability to characterize anomalous diffusion phenomena with fractional order behavior in time [19]. In biology and medicine, the equation is employed to model drug dispersion in tissues and describe cellular transport [12], providing insights into drug delivery system design and understanding particle movement within biological structures.

Environmental science benefits from the equation's use in studying contaminant transport in soil and groundwater, as well as in air pollution modeling, offering a more accurate representation of dispersion dynamics. In material science, the equation finds application in analyzing diffusion in porous media and studying phase transformations in materials [5]. Economics and finance benefit from modeling asset prices and financial indicators with fractional order diffusion, enhancing risk assessment in financial markets. Geophysics applications include investigating subsurface flow in underground reservoirs and understanding earthquake dynamics. The propagation of mechanical diffusive wave in viscoelastic media [29], random walk [7, 15] can also be modeled using fractional sub-diffusion equation. In telecommunications, the equation is utilized to analyze wireless communication signal propagation and network routing [4].

Finally, chemical engineering employs the equation to model reaction-diffusion processes and diffusion in catalytic systems, reflecting its versatility in addressing diverse diffusion-related phenomena [26, 31, 45]. So, the model problem

Received: 04 July 2023 ; Accepted: 06 March 2024.

* Corresponding author. Email: anshima.singh.rs.mat18@itbhu.ac.in.

considered here is the one-dimensional time-fractional Atangana-Baleanu diffusion equation describing subdiffusive phenomena with a non-homogeneous term

$$\begin{cases} {}_0^{ABC}\mathcal{D}_t^\mu v(y, t) = pv_{yy}(y, t) + F(y, t), & (y, t) \in \Omega, \\ v(y, 0) = G(y), & y \in [L_1, L_2], \\ v(L_1, t) = \alpha_1(t), & t \in [0, T], \\ v(L_2, t) = \alpha_2(t), & t \in [0, T], \end{cases} \quad (1.1)$$

where $0 < \mu \leq \frac{1}{2}$, $p > 0$, $\Omega := [L_1, L_2] \times [0, T]$, G , α_1 , α_2 are sufficiently smooth functions and ${}_0^{ABC}\mathcal{D}_t^\mu$ is as defined in section 2. When we deal with different definitions of fractional operators such as the Caputo operator, Grunwald-Letnikov operator, Riemann-Liouville operator, etc, we are faced with the problem of the singularity of kernels, due to which we cannot model many real-world problems. To overcome this drawback, Caputo and Fabrizio gave a new fractional operator, known as the Caputo-Fabrizio fractional operator, having a nonsingular kernel, but this derivative illustrates the localization problem [9]. To overcome this drawback, Atangana and Baleanu introduced a new definition, called Atangana-Baleanu-Caputo (ABC) fractional operator. There is a wide range of applications of the ABC fractional operator in the real world, and recent years this definition has revolutionized the field of fractional calculus. Due to the beauty and importance of the ABC fractional operator, researchers have been attracted to work with it. Ghanbari and Kumar [14] proposed a predator-prey model with the ABC operator. An important application of ABC fractional operator is related with non-linear fuzzy fractional differential equations [3]. Karaagac et al. [24] analyse the use of illicit drug with the ABC operator. In [46], the authors qualitatively and quantitatively analyse COVID-19 pandemic with the help of a mathematical model using the ABC fractional operator. A significant role of ABC fractional operator in the modeling of the hepatitis E virus is discussed in [33].

Cubic B-splines are considered to approximate different types of differential equations (see [10, 17, 20–22, 25, 41] and the references therein). Note that the undesirable inflexion points often arise, using piecewise cubic polynomial spline interpolation. Exponential splines generalize cubic splines and provide a solution to the issue of inflexion points. They offer distinct advantages over other spline types in certain applications. Their use of exponential basis functions allows for the creation of smooth curves with continuous derivatives, making them particularly well-suited for scenarios where a high degree of smoothness is essential. The local support property of exponential splines enables localized adjustments to the curve without affecting the entire spline, providing flexibility in modeling. Additionally, their efficient representation is characterized by a rapid decay of basis functions, allowing for a compact representation with fewer control points. The numerical stability associated with exponential functions can be advantageous in computational tasks. These characteristics, coupled with their widespread application in fields like computer-aided design and computer graphics, make exponential splines a valuable tool for capturing complex and visually appealing shapes. McCartin [30], Pruess [34, 35], and de Boor [8], studied the exponential splines thoroughly. There are a few papers available in the literature where exponential splines have been used to numerically solve different types of differential equations (see [23, 36, 38, 42, 43] and the references therein).

Analytical and numerical treatments of fractional sub-diffusion equations with different time fractional derivatives are considered in [11, 13, 16, 18, 27, 28, 50, 51], while the numerical treatment of the Atangana-Baleanu fractional sub-diffusion equation appears to be lacking. The superiority of exponential B-splines over cubic B-splines motivates us to use exponential B-splines to approximate the solution of problem (1.1). As far as we are aware (according to available literature), there is no result on approximations for Atangana-Baleanu fractional sub-diffusion equations based on exponential B-spline functions. Therefore, the main contribution in this paper is as follows:

- We develop a new method based on exponential B-splines to approximate the problem's solution (1.1).
- We prove that the proposed scheme is uniquely solvable and stable unconditionally.
- Convergence analysis of the method is rigorously discussed and error bounds in the maximum norm are obtained.
- Numerical simulations are done to show the accuracy and efficiency of the proposed scheme.

The remaining work is structured as follows. Section 2 includes some basic definitions from the fractional calculus. In section 3, we have given a brief description of the exponential B-spline functions that are helpful for the construction of the numerical scheme. After that, the numerical scheme is presented in this section. The theoretical analysis (stability and convergence) of the proposed method is discussed in detail in section 4. The numerical results of three test problems are given in section 5, which confirm our theoretical findings. Finally, a brief conclusion is provided in section 6.



2. SOME BASIC DEFINITIONS FROM FRACTIONAL CALCULUS

In this section, we discuss some definitions from fractional calculus.

Definition 2.1. Fractional integral of Riemann-Liouville type [32]

The Riemann-Liouville definition of fractional order integral of order $\mu > 0$ is given in the following way

$${}_a \mathcal{D}_t^{-\mu} \chi(t) = \frac{1}{\Gamma(\mu)} \int_a^t (t - \psi)^{\mu-1} \chi(\psi) d\psi, \quad t > 0.$$

Definition 2.2. Fractional operator of Riemann-Liouville type [32]

The Riemann-Liouville definition of fractional order derivative of order $\mu > 0$ is given in the following way

$${}^{RL} \mathcal{D}_t^\mu \chi(t) = \frac{1}{\Gamma(n - \mu)} \frac{d^n}{dt^n} \int_0^t (t - \psi)^{n-\mu-1} \chi(\psi) d\psi, \quad t > 0,$$

where $0 \leq n - 1 < \mu < n, n \in \mathbb{N}$.

Definition 2.3. Fractional operator of Caputo type [32]

The Caputo definition of fractional order derivative of order $\mu > 0$ is given in the following way

$${}_0^C \mathcal{D}_t^\mu \chi(t) = \begin{cases} \frac{1}{\Gamma(n-\mu)} \int_0^t (t-\psi)^{n-\mu-1} \chi^n(\psi) d\psi, & n-1 < \mu < n, \\ \frac{d^n \chi(t)}{dt^n}, & \mu = n \in \mathbb{N}. \end{cases}$$

Definition 2.4. Fractional operator of Caputo-Fabrizio type [9]

The Caputo-Fabrizio fractional derivative of the order $0 < \mu < 1$ is given in the following way

$${}_0^{CFC} \mathcal{D}_t^\mu \phi(y, t) = \frac{\mathcal{X}(\mu)}{(1-\mu)} \int_0^t \frac{\partial \phi(y, \psi)}{\partial \psi} \exp\left(\frac{-\mu}{1-\mu}(t-\psi)\right) d\psi,$$

where the normalization function $\mathcal{X}(\mu)$ meets the condition $\mathcal{X}(0) = \mathcal{X}(1) = 1$.

Definition 2.5. Fractional operator of ABC type [6]

The ABC fractional operator of order $0 < \mu < 1$ is given as

$${}_0^{ABC} \mathcal{D}_t^\mu v(y, t) = \frac{B(\mu)}{(1-\mu)} \int_0^t \frac{\partial v(y, \psi)}{\partial \psi} E_\mu\left(\frac{-\mu}{1-\mu}(t-\psi)^\mu\right) d\psi, \tag{2.1}$$

where $B(\mu)$ is the normalization function meets the conditions $B(0) = B(1) = 1$ and $E_\mu(\Psi)$ is the one-parameter Mittag-Leffler function defined by [32]

$$E_\mu(\Psi) = \sum_{l=0}^{\infty} \frac{\Psi^l}{\Gamma(\mu l + 1)},$$

where $\mu > 0, \Psi \in \mathbb{C}$, and Γ denotes the Euler Gamma function. Also, the two parameter Mittag-Leffler function is defined by [32]

$$E_{\mu,\gamma}(\Psi) = \sum_{l=0}^{\infty} \frac{\Psi^l}{\Gamma(\mu l + \gamma)}, \tag{2.2}$$

where $\mu > 0, \gamma \in \mathbb{R}$, and $\Psi \in \mathbb{C}$.

3. NUMERICAL SCHEME

The numerical scheme designed for the fractional sub-diffusion equation with ABC time fractional operator is presented in this section. Let $D_y : L_1 = y_0 < y_1 < \dots < y_{M-1} < y_M = L_2$ and $D_t : 0 = t_0 < t_1 < \dots < t_{N-1} < t_N = T$ be uniform partitions of $[L_1, L_2]$ and $[0, T]$ respectively. Denote $h_y = \frac{(L_2-L_1)}{M}$ and $h_t = \frac{T}{N}$, where h_y and h_t are the mesh spacing in the spatial and temporal directions respectively.



3.1. Discretization of the ABC fractional operator. Here we first approximate the ABC time fractional operator at t_n , $n = 0, 1, \dots, N$, following [49] as follows

$$\begin{aligned} [{}^{\text{ABC}}_0 \mathcal{D}_t^\mu v(y, t)]_{t=t_n} &= \frac{B(\mu)}{(1-\mu)} \int_{t_0}^{t_n} \frac{\partial v(y, \psi)}{\partial \psi} E_\mu \left[\frac{-\mu}{1-\mu} (t_n - \psi)^\mu \right] d\psi \\ &= \frac{B(\mu)}{(1-\mu)} \sum_{l=0}^{n-1} \int_{t_l}^{t_{l+1}} \frac{v(y, t_{l+1}) - v(y, t_l)}{h_t} E_\mu \left[\frac{-\mu}{1-\mu} (t_n - \psi)^\mu \right] d\psi + \mathcal{T}^n \\ &= \frac{B(\mu)}{(1-\mu)} \sum_{l=0}^n S_l^n v(y, t_l) + \mathcal{T}^n, \end{aligned} \quad (3.1)$$

where the coefficients S_l^n are given as

$$S_l^n = \begin{cases} (n-1)E_{\mu,2} \left(\frac{-\mu}{1-\mu} (n-1)^\mu h_t^\mu \right) - nE_{\mu,2} \left(\frac{-\mu}{1-\mu} n^\mu h_t^\mu \right), & l=0, \\ (n-l+1)E_{\mu,2} \left(\frac{-\mu}{1-\mu} (n-l+1)^\mu h_t^\mu \right) - 2(n-l)E_{\mu,2} \left(\frac{-\mu}{1-\mu} (n-l)^\mu h_t^\mu \right) \\ + (n-l-1)E_{\mu,2} \left(\frac{-\mu}{1-\mu} (n-l-1)^\mu h_t^\mu \right), & 0 < l < n, \\ E_{\mu,2} \left(\frac{-\mu}{1-\mu} h_t^\mu \right), & l=n, \end{cases} \quad (3.2)$$

and the truncation error \mathcal{T}^n is bounded by

$$\mathcal{T}^n \leq \frac{c^* B(\mu) h_t^2}{(1-\mu) 2} \left[\max_{t_0 \leq t \leq t_{n-1}} \left| \frac{\partial^2 v(y, t)}{\partial t^2} \right| \right], \quad (3.3)$$

where c^* is a positive constant.

Lemma 3.1. *The coefficients S_k^n defined in Equation (3.2) satisfy*

- (a). $S_k^n \leq 0$, $0 \leq k \leq n-1$,
- (b). $S_n^n > 0$,
- (c). $\sum_{k=0}^{n-1} S_k^n = -S_n^n$.

Proof. The inequality (a) can be proved following [48, Lemma 2]. Next, for the inequality (b) we have

$$S_n^n = E_{\mu,2} \left(\frac{-\mu}{1-\mu} h_t^\mu \right), \quad (3.4)$$

which on using (2.2) leads to

$$\begin{aligned} S_n^n &= \sum_{i=0}^{\infty} \frac{(-1)^i \left(\frac{\mu}{1-\mu} h_t^\mu \right)^i}{\Gamma(\mu i + 2)} \\ &= \left(1 - \frac{\left(\frac{\mu}{1-\mu} h_t^\mu \right)}{\Gamma(\mu + 2)} \right) + \left(\frac{\left(\frac{\mu}{1-\mu} h_t^\mu \right)^2}{\Gamma(2\mu + 2)} - \frac{\left(\frac{\mu}{1-\mu} h_t^\mu \right)^3}{\Gamma(3\mu + 2)} \right) + \dots \end{aligned}$$

Now, for $i \in \{0\} \cup \mathbb{N}$, we have

$$\frac{\left(\frac{\mu}{1-\mu} h_t^\mu \right)^{i+1}}{\Gamma(\mu(i+1) + 2)} < \frac{\left(\frac{\mu}{1-\mu} h_t^\mu \right)^i}{\Gamma(\mu i + 2)}, \quad (3.5)$$

since $\Gamma(z)$ is an increasing function in $[\alpha, \infty)$, $\alpha \in (1, 2)$ and using the assumption $0 < h_t^\mu < \left(\frac{1}{\mu} - 1 \right)$, which is not restrictive at all. Therefore, using (3.5), we have $S_n^n > 0$.



Further, to prove (c) we call $\phi(l) = E_{\mu,2} \left(\frac{-\mu}{1-\mu} l^\mu h_t^\mu \right)$, and proceed as follows

$$\begin{aligned} \sum_{k=0}^{n-1} S_k^n &= S_0^n + S_1^n + S_2^n + \dots + S_{n-3}^n + S_{n-2}^n + S_{n-1}^n \\ &= [(n-1)\phi(n-1) - n\phi(n)] + [n\phi(n) - 2(n-1)\phi(n-1) + (n-2)\phi(n-2)] \\ &\quad + [(n-1)\phi(n-1) - 2(n-2)\phi(n-2) + (n-3)\phi(n-3)] + \dots + [4\phi(4) \\ &\quad - 2(3\phi(3)) + 2\phi(2)] + [3\phi(3) - 2(2\phi(2)) + \phi(1)] + [2\phi(2) - 2\phi(1)] \\ &= -\phi(1) = -S_n^n. \end{aligned}$$

This completes the proof. □

Now using approximation of ABC time-fractional operator from Eq. (3.1) in Eq. (1.1) we get

$$S_n^n v^n = - \sum_{k=0}^{n-1} S_k^n v^k + \frac{p(1-\mu)}{B(\mu)} \frac{\partial^2 v^n}{\partial x^2} + \frac{(1-\mu)}{B(\mu)} F^n.$$

Thus, we get the time semi-discrete problem as follows

$$L_y v^n = - \sum_{k=0}^{n-1} S_k^n v^k + \frac{(1-\mu)}{B(\mu)} F^n, \tag{3.6}$$

with

$$\begin{cases} v^0(y) = G(y), & x \in [L_1, L_2], \\ v^n(L_1) = \alpha_1^n, & 0 \leq n \leq N, \\ v^n(L_2) = \alpha_2^n, & 0 \leq n \leq N, \end{cases} \tag{3.7}$$

where

$$\begin{aligned} L_y &= S_n^n I - \frac{p(1-\mu)}{B(\mu)} \frac{\partial^2}{\partial x^2}, \\ F^n &= F(y, t_n), \\ \alpha_1^n &= \alpha_1(t_n), \\ \alpha_2^n &= \alpha_2(t_n). \end{aligned}$$

Here, v^n approximates $v(y, t)$ at t_n .

3.2. Exponential B-spline functions. We define the exponential B-spline functions $\mathcal{B}_i(y)$ on the partition D_y along with six extra nodes $y_m, -3 \leq m \leq M + 3$, which are ghost points beyond the interval $[L_1, L_2]$. Taking ρ as a non-negative parameter, let us denote

$$\begin{aligned} s &= \sinh(\rho h_y), \\ c &= \cosh(\rho h_y), \end{aligned}$$

The exponential B-spline functions $\mathcal{B}_i(y)$ are defined as follows [30]

$$\mathcal{B}_i(y) = \begin{cases} \mathcal{E}(y_{i-2} - y) - \frac{\mathcal{E}}{\rho} \sinh(\rho(y_{i-2} - y)), & y \in [y_{i-2}, y_{i-1}], \\ a' + b'(y_i - y) + c' e^{\rho(y_i - y)} + d' e^{-\rho(y_i - y)}, & y \in [y_{i-1}, y_i], \\ a' + b'(y - y_i) + c' e^{\rho(y - y_i)} + d' e^{-\rho(y - y_i)}, & y \in [y_i, y_{i+1}], \\ \mathcal{E}(y - y_{i+2}) - \frac{\mathcal{E}}{\rho} \sinh(\rho(y - y_{i+2})), & y \in [y_{i+1}, y_{i+2}], \\ 0, & \text{else,} \end{cases} \tag{3.8}$$

where $-1 \leq i \leq M + 1$, and

$$\mathcal{E} = \frac{\rho}{2(\rho h_y c - s)}, \quad a' = \frac{\rho h_y c}{\rho h_y c - s}, \quad b' = \frac{\rho}{2} \left[\frac{c(c-1) + s^2}{(\rho h_y c - s)(1-c)} \right],$$



$$c' = \frac{1}{4} \left[\frac{e^{-\rho h_y}(1-c) + s(e^{-\rho h_y} - 1)}{(\rho h_y c - s)(1-c)} \right],$$

$$d' = \frac{1}{4} \left[\frac{e^{\rho h_y}(c-1) + s(e^{\rho h_y} - 1)}{(\rho h_y c - s)(1-c)} \right].$$

At every mesh point, the values of $\mathcal{B}_i(y)$, $\mathcal{B}'_i(y)$, and $\mathcal{B}''_i(y)$ given as following

$$\mathcal{B}_i(y_j) = \begin{cases} 1, & \text{if } j = i, \\ \frac{s - \rho h_y}{2(\rho h_y c - s)}, & \text{if } j = i \pm 1, \\ 0, & \text{otherwise.} \end{cases}$$

$$\mathcal{B}'_i(y_j) = \begin{cases} 0, & \text{if } j = i, \\ \frac{\mp \rho(c-1)}{2(\rho h_y c - s)}, & \text{if } j = i \pm 1, \\ 0, & \text{otherwise.} \end{cases} \quad (3.9)$$

$$\mathcal{B}''_i(y_j) = \begin{cases} \frac{-\rho^2 s}{\rho h_y c - s}, & \text{if } j = i, \\ \frac{\rho^2 s}{2(\rho h_y c - s)}, & \text{if } j = i \pm 1, \\ 0, & \text{otherwise.} \end{cases}$$

The exponential B-spline functions $\{\mathcal{B}_i(y)\}_{i=-1}^{M+1} \in C^2(\mathbb{R})$. The set $\{\mathcal{B}_i(y)\}_{i=-1}^{M+1}$ makes a basis for the exponential B-spline space W_{M+3} over the interval $[L_1, L_2]$.

3.3. Fully discrete Exponential B-spline scheme. Let us consider $\mathcal{V}^n(y)$ be the approximate solution of problem (3.6) and (3.7) at the n th time level given as

$$\mathcal{V}^n(y) = \sum_{m=-1}^{M+1} \mathcal{C}_m^n \mathcal{B}_m(y), \quad (3.10)$$

where the unknown coefficients \mathcal{C}_m^n are required to be determined. Further, we get the values of $\mathcal{V}^n(y_m)$, $\mathcal{V}_y^n(y_m)$, and $\mathcal{V}_{yy}^n(y_m)$ for $m = 0, 1, \dots, M$ using (3.9) having \mathcal{C}_m^n in the following manner

$$\mathcal{V}^n(y_m) = q\mathcal{C}_{m-1}^n + \mathcal{C}_m^n + q\mathcal{C}_{m+1}^n, \quad (3.11)$$

$$\mathcal{V}_y^n(y_m) = \bar{e}(c-1)[\mathcal{C}_{m+1}^n - \mathcal{C}_{m-1}^n], \quad (3.12)$$

$$\mathcal{V}_{yy}^n(y_m) = \bar{q}[\mathcal{C}_{m-1}^n - 2\mathcal{C}_m^n + \mathcal{C}_{m+1}^n], \quad (3.13)$$

where

$$q = \frac{s - \rho h_y}{2(\rho h_y c - s)}, \quad \bar{e} = \frac{\rho}{2(\rho h_y c - s)}, \quad \bar{q} = \frac{\rho^2 s}{2(\rho h_y c - s)}.$$

Now, using the approximation (3.10) in Eqs. (3.6) and (3.7) at $y = y_m$ yield

$$S_n^n \mathcal{V}^n(y_m) = - \sum_{k=0}^{n-1} S_k^n \mathcal{V}^k(y_m) + \frac{p(1-\mu)}{B(\mu)} \frac{\partial^2 \mathcal{V}^n(y_m)}{\partial x^2} + \frac{(1-\mu)}{B(\mu)} F^n(y_m), \quad (3.14)$$

with

$$\begin{cases} \mathcal{V}^0(y_m) = G(y_m), & 0 \leq m \leq M, \\ \mathcal{V}^n(y_0) = \alpha_1^n, & 0 \leq n \leq N, \\ \mathcal{V}^n(y_M) = \alpha_2^n, & 0 \leq n \leq N. \end{cases} \quad (3.15)$$

Further substituting the Eqs. (3.11) and (3.13) in Eqs. (3.14) and (3.11) in Eq. (3.15), we have

$$\begin{aligned} & (S_n^n q - d)\mathcal{C}_{m-1}^n + (S_n^n + 2d)\mathcal{C}_m^n + (S_n^n q - d)\mathcal{C}_{m+1}^n \\ & = -S_0^n (q\mathcal{C}_{m-1}^0 + \mathcal{C}_m^0 + q\mathcal{C}_{m+1}^0) - \sum_{k=1}^{n-1} S_k^n (q\mathcal{C}_{m-1}^k + \mathcal{C}_m^k + q\mathcal{C}_{m+1}^k) + d_1 F_m^n, \quad (0 \leq m \leq M, 0 \leq n \leq N), \end{aligned} \quad (3.16)$$



and

$$q\mathcal{C}_{-1}^n = \alpha_1^n - \mathcal{C}_0^n - q\mathcal{C}_1^n, \tag{3.17}$$

$$q\mathcal{C}_{M+1}^n = \alpha_2^n - \mathcal{C}_M^n - q\mathcal{C}_{M-1}^n, \tag{3.18}$$

where

$$d = \frac{p(1-\mu)}{B(\mu)}\bar{q}, \quad d_1 = \frac{(1-\mu)}{B(\mu)}.$$

The unknown coefficients \mathcal{C}_{-1}^n and \mathcal{C}_{M+1}^n can be eliminated in system (3.16) using the Eqs. (3.17) and (3.18), respectively. Finally, a tri-diagonal system of order $(M + 1)$ for each n is obtained

$$A\mathcal{C}^n = B \left(-S_0^n \mathcal{C}^0 - \sum_{k=1}^{n-1} S_k^n \mathcal{C}^k \right) + R, \tag{3.19}$$

where

$$A = \begin{pmatrix} d(2 + \frac{1}{q}) & 0 & 0 & \dots & 0 & 0 & 0 \\ (S_n^n q - d) & (S_n^n + 2d) & (S_n^n q - d) & \dots & 0 & 0 & 0 \\ 0 & (S_n^n q - d) & (S_n^n + 2d) & \dots & 0 & 0 & 0 \\ & & & \dots & & & \\ 0 & 0 & 0 & \dots & (S_n^n + 2d) & (S_n^n q - d) & 0 \\ 0 & 0 & 0 & \dots & (S_n^n q - d) & (S_n^n + 2d) & (S_n^n q - d) \\ 0 & 0 & 0 & \dots & 0 & 0 & d(2 + \frac{1}{q}) \end{pmatrix},$$

$$\mathcal{C}^n = \begin{pmatrix} \mathcal{C}_0^n \\ \mathcal{C}_1^n \\ \vdots \\ \vdots \\ \mathcal{C}_{M-1}^n \\ \mathcal{C}_M^n \end{pmatrix}, \quad B = \begin{pmatrix} 0 & 0 & 0 & \dots & 0 & 0 & 0 \\ q & 1 & q & \dots & 0 & 0 & 0 \\ 0 & q & 1 & \dots & 0 & 0 & 0 \\ & & & \dots & & & \\ 0 & 0 & 0 & \dots & 1 & q & 0 \\ 0 & 0 & 0 & \dots & q & 1 & q \\ 0 & 0 & 0 & \dots & 0 & 0 & 0 \end{pmatrix},$$

and

$$R = \begin{pmatrix} d_1 F_0^n - \sum_{k=0}^{n-1} S_k^n \alpha_1^k - \frac{1}{q}(S_n^n q - d)\alpha_1^n \\ d_1 F_1^n \\ d_1 F_2^n \\ \vdots \\ \vdots \\ d_1 F_{M-1}^n \\ d_1 F_M^n - \sum_{k=0}^{n-1} S_k^n \alpha_2^k - \frac{1}{q}(S_n^n q - d)\alpha_2^n \end{pmatrix}.$$

It is clear that the systems in (3.19) for $0 \leq n \leq N$, can be solved recursively after knowing the initial vector \mathcal{C}^0 . Further, notice that \mathcal{C}_{-1}^0 and \mathcal{C}_{M+1}^0 can be then evaluated using Eqs. (3.17) and (3.18) respectively.

3.4. Initial vector estimation. From the initial condition given in (1.1), we have

$$\mathcal{Y}_y(L_1, 0) = G'(L_1), \quad \mathcal{Y}_y(L_2, 0) = G'(L_2).$$

Using Equation (3.12) in above equations

$$\mathcal{Y}_y(y_0, 0) = \mathcal{Y}_y(L_1, 0) = \bar{e}(c - 1)[\mathcal{C}_1^0 - \mathcal{C}_{-1}^0] = G'(L_1), \tag{3.20}$$

$$\mathcal{Y}_y(y_M, 0) = \mathcal{Y}_y(L_2, 0) = \bar{e}(c - 1)[\mathcal{C}_{M+1}^0 - \mathcal{C}_{M-1}^0] = G'(L_2). \tag{3.21}$$

We get an algebraic system of $(M + 1)$ equations by substituting relation (3.11) into initial condition given in Equation (1.1)

$$\mathcal{Y}(y_m, 0) = q\mathcal{C}_{m-1}^0 + \mathcal{C}_m^0 + q\mathcal{C}_{m+1}^0 = G(y_m), \quad m = 0, 1, \dots, M, \tag{3.22}$$



with unknowns $\mathcal{C}_{-1}^0, \mathcal{C}_0^0, \mathcal{C}_1^0, \dots, \mathcal{C}_{M-1}^0, \mathcal{C}_M^0, \mathcal{C}_{M+1}^0$. Here, \mathcal{C}_{-1}^0 and \mathcal{C}_{M+1}^0 can be eliminated using Equations (3.20) and (3.21) respectively. Thus, we get

$$D\mathcal{C}^0 = Q, \quad (3.23)$$

where

$$D = \begin{pmatrix} 1 & 2q & 0 & \dots & 0 & 0 & 0 \\ q & 1 & q & \dots & 0 & 0 & 0 \\ 0 & q & 1 & \dots & 0 & 0 & 0 \\ & & & \dots & & & \\ 0 & 0 & 0 & \dots & 1 & q & 0 \\ 0 & 0 & 0 & \dots & q & 1 & q \\ 0 & 0 & 0 & \dots & 0 & 2q & 1 \end{pmatrix},$$

$$\mathcal{C}^0 = \begin{pmatrix} \mathcal{C}_0^0 \\ \mathcal{C}_1^0 \\ \vdots \\ \mathcal{C}_{M-1}^0 \\ \mathcal{C}_M^0 \end{pmatrix}, \quad Q = \begin{pmatrix} G(y_0) + \frac{q}{\bar{e}(c-1)}G'(L_1) \\ G(y_1) \\ \vdots \\ G(y_{M-1}) \\ G(y_M) - \frac{q}{\bar{e}(c-1)}G'(L_2) \end{pmatrix}.$$

4. THEORETICAL ANALYSIS

Here we will discuss the theoretical analysis which includes stability and convergence of the proposed numerical method.

Lemma 4.1. *The coefficient matrices A and D are strictly diagonally dominant, and hence the method provides a unique solution.*

Proof. We have

$$\begin{aligned} |(S_n^n + 2d)| - 2|(S_n^n q - d)| &= S_n^n + 2d - 2|S_n^n q - d| \\ &\geq S_n^n + 2d - 2(S_n^n q + d) \quad (\because 2|S_n^n q - d| \leq 2S_n^n q + 2d) \\ &= S_n^n(1 - 2q). \end{aligned}$$

We also have $(1 - 2q) > 0$, as can be easily checked, since it is $(s - \rho h_y) > 0$, $(\rho h_y c - s) > 0$, and $(s - \rho h_y) < (\rho h_y c - s)$. This can be verified by taking the series expansions of $\cosh(y)$ and $\sinh(y)$. Further, we note that $S_n^n > 0$ from Lemma 3.1. Therefore, we get

$$|(S_n^n + 2d)| - 2|(S_n^n q - d)| > 0.$$

Thus, the matrix A is strictly diagonally dominant. It is also evident that matrix D is strictly diagonally dominant. This completes the proof. \square

4.1. Stability analysis.

Theorem 4.1.1. The numerical scheme (3.16) is unconditionally stable.

Proof. We will show the stability of proposed scheme using the von Neumann method.

Let the system (3.16) having a perturbed solution $\bar{\mathcal{C}}$, then we will examine how the perturbation $\psi_m^n = \mathcal{C}_m^n - \bar{\mathcal{C}}_m^n$ evolves over time. Note that ψ_m^n satisfies the following equation

$$\begin{aligned} (S_n^n q - d)\psi_{m-1}^n + (S_n^n + 2d)\psi_m^n + (S_n^n q - d)\psi_{m+1}^n \\ = -S_0^n(q\psi_{m-1}^0 + \psi_m^0 + q\psi_{m+1}^0) - \sum_{k=1}^{n-1} S_k^n(q\psi_{m-1}^k + \psi_m^k + q\psi_{m+1}^k). \end{aligned} \quad (4.1)$$

Now, we assume that

$$\psi_m^n = \eta^n e^{i\eta m h_y}, \quad (4.2)$$



where η is the wave number and $i = \sqrt{-1}$. Putting the Eq. (4.2) in (4.1) gives

$$\eta^n = -\mathscr{W}^n \sum_{k=0}^{n-1} S_k^n \eta^k, \tag{4.3}$$

where

$$\mathscr{W}^n = \frac{1 + 2q \cos(\eta h_y)}{S_n^n (1 + 2q \cos(\eta h_y)) + 2d(1 - \cos(\eta h_y))}$$

is a non-negative value.

With the help of mathematical induction, we show that $|\eta^n| \leq |\eta^0|$. For $n = 1$, we have

$$\begin{aligned} |\eta^1| &= |-\mathscr{W}^1 S_0^1 \eta^0| \\ &= |\mathscr{W}^1 S_1^1 \eta^0|, \quad (\because S_0^1 = -S_1^1). \end{aligned}$$

Using Lemma 3.1, we have $|\mathscr{W}^1 S_1^1| \leq 1$. Therefore, $|\eta^1| \leq |\eta^0|$. Moreover, we suppose that

$$|\eta^j| \leq |\eta^0|, \quad 1 \leq j \leq n - 1. \tag{4.4}$$

Again, using Lemma 3.1 with the assumption (4.4), the Equation (4.3) leads to

$$\begin{aligned} |\eta^n| &= \left| -\mathscr{W}^n \sum_{k=0}^{n-1} S_k^n \eta^k \right| \\ &\leq |\mathscr{W}^n| \left| \sum_{k=0}^{n-1} -S_k^n \right| \max_{0 \leq k \leq n-1} |\eta^k| \\ &\leq |\mathscr{W}^n| |S_n^n| |\eta^0|. \end{aligned}$$

Using Lemma 3.1, it can be easily seen that $|\mathscr{W}^n S_n^n| \leq 1$, and consequently,

$$|\eta^n| \leq |\eta^0|, \forall n.$$

Thus, we see that the perturbation is bounded unconditionally at every time level. □

4.2. Convergence analysis. We now provide the error bounds of the proposed numerical method by using the procedure adopted in [37, 38, 43]. We shall use the following results.

Lemma 4.2. [36] The elements of the base $\{\mathcal{B}_m(y)\}_{m=-1}^{M+1}$ of W_{M+3} (the exponential B-spline space), meet the following inequality

$$\sum_{m=-1}^{M+1} |\mathcal{B}_m(y)| \leq \frac{5}{2}, \quad L_1 \leq y \leq L_2.$$

Theorem 4.2.1. [34] Let $\tilde{V}^n(y)$ be a unique exponential B-spline interpolant to the solution $v^n(y)$ of problem (3.6)-(3.7). If $v^n \in C^4([L_1, L_2])$ and $F^n \in C^2([L_1, L_2])$ then there exist constants k_i such that

$$\left\| \frac{\partial^j}{\partial y^j} \left(v^n(y) - \tilde{V}^n(y) \right) \right\|_{t_\infty} \leq k_j h_y^{4-i}, \quad j = 0, 1, 2.$$

Theorem 4.2.2. Let $\mathscr{V}^n(y)$ be the exponential B-spline collocation approximation in (3.10) to the solution $v(y, t_n)$ of the time-fractional sub-diffusion Equations (1.1). If $v \in C^{4,0}(\Omega)$ and $F \in C^{2,0}(\Omega)$, then for each t_n there exist positive constants c_1 and c_2 such that

$$\|v(y, t_n) - \mathscr{V}^n(y)\|_\infty \leq c_1 h_y^2 + c_2 h_t^2.$$

Proof. Let $\tilde{V}^n(y)$ be the unique exponential B-spline interpolant to the exact solution $v^n(y)$ of the problem (3.6)-(3.7) given by

$$\tilde{V}^n(y) = \sum_{m=-1}^{M+1} \delta_m^n \mathcal{B}_m(y). \tag{4.5}$$



TABLE 1. Errors \mathcal{L}_2 , \mathcal{L}_∞ and corresponding experimental orders of convergence ${}_y EOC_2$, ${}_y EOC_\infty$ with $N = 500$, $\rho = 1$ for Example 5.1.

μ	M	\mathcal{L}_2 - error	${}_y EOC_2$	\mathcal{L}_∞ - error	${}_y EOC_\infty$
0.2	2	$1.2444e-01$		$1.7598e-01$	
	2^2	$3.5049e-02$	1.8280	$4.9566e-02$	1.8280
	2^3	$8.9849e-03$	1.9638	$1.2707e-02$	1.9638
	2^4	$2.2598e-03$	1.9913	$3.1958e-03$	1.9913
	2^5	$5.6578e-04$	1.9979	$8.0014e-04$	1.9979
	2^6	$1.4149e-04$	1.9995	$2.0010e-04$	1.9995
0.3	2	$1.2401e-01$		$1.7538e-01$	
	2^2	$3.4912e-02$	1.8287	$4.9372e-02$	1.8287
	2^3	$8.9484e-03$	1.9640	$1.2655e-02$	1.9640
	2^4	$2.2505e-03$	1.9914	$3.1827e-03$	1.9914
	2^5	$5.6345e-04$	1.9979	$7.9684e-04$	1.9979
	2^6	$1.4090e-04$	1.9996	$1.9926e-04$	1.9996
0.5	2	$1.2260e-01$		$1.7338e-01$	
	2^2	$3.4451e-02$	1.8313	$4.8722e-02$	1.8313
	2^3	$8.8259e-03$	1.9647	$1.2482e-02$	1.9647
	2^4	$2.2194e-03$	1.9916	$3.1387e-03$	1.9916
	2^5	$5.5562e-04$	1.9980	$7.8576e-04$	1.9980
	2^6	$1.3892e-04$	1.9999	$1.9646e-04$	1.9999

Now the problem (3.6)-(3.7) can be rewritten in the following form

$$L_y v^n = \mathcal{F}, \quad v^n(L_1) = \alpha_1^n, \quad v^n(L_2) = \alpha_2^n, \quad (4.6)$$

where

$$\mathcal{F} = - \sum_{k=0}^{n-1} S_k^n v^k + \frac{(1-\mu)}{B(\mu)} F^n. \quad (4.7)$$

From Theorem 4.2.1 and [32, Theorem 1.6, p.35] it is clear that

$$|L_y(v^n(y_m) - \tilde{V}^n(y_m))| \leq \beta h_y^2, \quad 0 \leq n \leq N, \quad 0 \leq m \leq M,$$

where $\beta = k_0 C h_y^2 + \frac{p(1-\mu)}{B(\mu)} k_2$. Thus,

$$\|L_y(v^n(y_m) - \tilde{V}^n(y_m))\|_\infty \leq \beta h_y^2, \quad \forall n. \quad (4.8)$$

At n th-time level, we can write

$$L_y \tilde{V}^n(y_m) = L_y v^n(y_m) + \tilde{f}^n(y_m), \quad 0 \leq m \leq M, \quad (4.9)$$

$$\tilde{V}^n(y_0) = v^n(y_0) + \tilde{\alpha}_1^n, \quad (4.10)$$

$$\tilde{V}^n(y_M) = v^n(y_M) + \tilde{\alpha}_2^n, \quad (4.11)$$



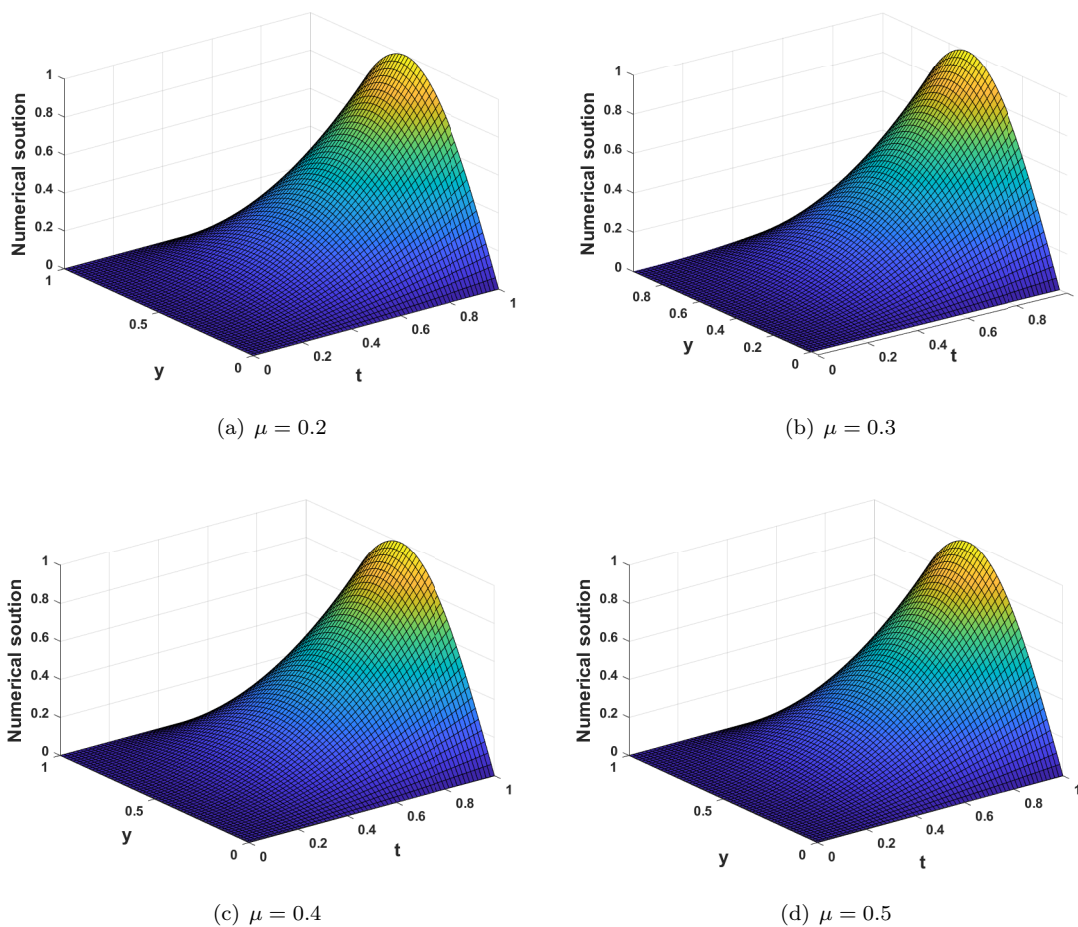


FIGURE 1. Numerical solution of Example 5.1 with $M = N = 60$ and $\rho = 1$.

where \tilde{f}^n is an error function of order $O(h_y^2)$, and $\tilde{\alpha}_1^n, \tilde{\alpha}_2^n$ are error functions with order $O(h_y^4)$. Since $v^n(y_m) = \mathcal{V}^n(y_m), 0 \leq m \leq M$, therefore we can write the system (4.9)-(4.11) as

$$A\delta^n = A\mathcal{E}^n + \mathcal{D}^n, \tag{4.12}$$

where

$$\mathcal{D}^n = [\tilde{f}^n(y_0), \tilde{f}^n(y_1), \dots, \tilde{f}^n(y_M)]^T - [(S_n^n - d/q)\tilde{\alpha}_1^n, 0, \dots, 0, (S_n^n - d/q)\tilde{\alpha}_2^n]^T.$$

Above equation yields

$$\|\mathcal{D}^n\|_\infty \leq C_1 h_y^2 + C_2 |(S_n^n - d/q)| h_y^4 \leq \lambda h_y^2, \tag{4.13}$$

here, C_1, C_2 and λ are positive constants. Now from equation (4.12) we have

$$A(\delta^n - \mathcal{E}^n) = \mathcal{D}^n. \tag{4.14}$$

Thus,

$$\|(\delta^n - \mathcal{E}^n)\|_\infty \leq \|A^{-1}\|_\infty \|\mathcal{D}^n\|_\infty. \tag{4.15}$$



From Lemma 4.1, matrix A is strictly diagonally dominant, therefore it is invertible. Further $(|A_{i,i}| - \sum_{i \neq j} |A_{i,j}|) > \nu > 0$, hence from [47]

$$\|A^{-1}\|_\infty \leq \frac{1}{\nu}, \tag{4.16}$$

Thus, using Equations (4.13) and (4.16) in Equation (4.15), we have

$$\|\delta^n - \mathcal{C}^n\|_\infty \leq \frac{\lambda}{\nu} h_y^2, \quad 1 \leq n \leq N, \tag{4.17}$$

where $\|\delta^n - \mathcal{C}^n\|_\infty = \max_{0 \leq m \leq M} (|\delta_m^n - \mathcal{C}_m^n|)$.

Moreover Equations (4.10) and (4.11) give

$$|\delta_{-1}^n - \mathcal{C}_{-1}^n| \leq \hat{d} h_y^2 \quad \text{and} \quad |\delta_{M+1}^n - \mathcal{C}_{M+1}^n| \leq \hat{d} h_y^2, \tag{4.18}$$

where \hat{d} is a constant. Hence from Equations (4.17) and (4.18) we finally get

$$\max_{-1 \leq m \leq M+1} (|\delta_m^n - \mathcal{C}_m^n|) \leq \tilde{d} h_y^2, \quad n = 1, 2, \dots, N, \tag{4.19}$$

where $\tilde{d} = \max\{\lambda/\nu, \hat{d}\}$. Next take

$$\begin{aligned} \tilde{V}^n(y) - \mathcal{V}^n(y) &= \sum_{m=-1}^{M+1} (\delta_m^n - \mathcal{C}_m^n) \mathcal{B}_m(y). \\ |\tilde{V}^n(y_i) - \mathcal{V}^n(y_i)| &\leq \max_{-1 \leq m \leq M+1} (|\delta_m^n - \mathcal{C}_m^n|) \sum_{m=-1}^{M+1} |\mathcal{B}_m(y_i)|, \quad 0 \leq i \leq M. \end{aligned}$$

Now above relation with Lemma 4.2 and inequality (4.19) provides

$$\|\tilde{V}^n - \mathcal{V}^n\|_\infty \leq \frac{5}{2} \tilde{d} h_y^2. \tag{4.20}$$

Using the triangle inequality we get

$$\|v^n - \mathcal{V}^n\|_\infty \leq \|v^n - \tilde{V}^n\|_\infty + \|\tilde{V}^n - \mathcal{V}^n\|_\infty. \tag{4.21}$$

Now Theorem 4.2.1 together with inequality (4.20) provide

$$\|v^n - \mathcal{V}^n\|_\infty \leq l h_y^2,$$

where $l = k_0 h_y^2 + \frac{5}{2} \tilde{d}$. Now, the above inequality combined with the relation (3.3) prove the theorem. \square

5. NUMERICAL RESULTS

This section is devoted to show the numerical results for three test examples that are in full support of the theoretical. If $v(y_m, t_n)$ and $\mathcal{V}(y_m, t_n)$ are, respectively, the exact and the approximate solution of problem (1.1) at (y_m, t_n) then the following norms will be used to measure the authenticity of the numerical method

$$\mathcal{L}_\infty(M, N) = \|v(y_m, t_n) - \mathcal{V}(y_m, t_n)\|_\infty = \max_{1 \leq n \leq N} \max_{1 \leq m \leq M-1} |v(y_m, t_n) - \mathcal{V}(y_m, t_n)|, \tag{5.1}$$

$$\mathcal{L}_2(M, N) = \|v(y_m, t_n) - \mathcal{V}(y_m, t_n)\|_2 = \max_{1 \leq n \leq N} \sqrt{h_y \sum_{m=1}^{M-1} (v(y_m, t_n) - \mathcal{V}(y_m, t_n))^2}. \tag{5.2}$$

The convergence order (EOC) is evaluated by the following formulas

$${}_tEOC_2 = \log_2 \left(\frac{\mathcal{L}_2(M, N)}{\mathcal{L}_2(M, 2N)} \right), \quad {}_tEOC_\infty = \log_2 \left(\frac{\mathcal{L}_\infty(M, N)}{\mathcal{L}_\infty(M, 2N)} \right), \tag{5.3}$$

$${}_yEOC_2 = \log_2 \left(\frac{\mathcal{L}_2(M, N)}{\mathcal{L}_2(2M, N)} \right), \quad {}_yEOC_\infty = \log_2 \left(\frac{\mathcal{L}_\infty(M, N)}{\mathcal{L}_\infty(2M, N)} \right). \tag{5.4}$$



TABLE 2. Comparison with method in [49] taking $N = 500$ for Example 5.1.

α	M	Present method		Method in [49]	
		\mathcal{L}_∞ - error	${}_xO_{\mathcal{L}_\infty}$	\mathcal{L}_∞ - error	${}_xO_{\mathcal{L}_\infty}$
0.2	10	1.9059e-03	-	7.4567e-03	-
	20	4.7686e-04	1.9988	1.8585e-03	2.0044
	40	1.1923e-04	1.9998	4.6432e-04	2.0009
	80	2.9799e-05	2.0004	1.1613e-04	1.9994
	160	7.4398e-06	2.0019	2.9100e-05	1.9966
0.3	10	1.8981e-03	-	7.4049e-03	-
	20	4.7488e-04	1.9989	1.8457e-03	2.0043
	40	1.1873e-04	1.9999	4.6120e-04	2.0007
	80	2.9663e-05	2.0009	1.1540e-04	1.9987
	160	7.3960e-06	2.0038	2.8978e-05	1.9937

TABLE 3. Errors \mathcal{L}_2 , \mathcal{L}_∞ and corresponding experimental order of convergences ${}_{\text{t}}EOC_2$, ${}_{\text{t}}EOC_\infty$ with $M = 10^3$, $\rho = 1$ for Example 5.1.

μ	N	\mathcal{L}_2 - error	${}_{\text{t}}EOC_2$	\mathcal{L}_∞ - error	${}_{\text{t}}EOC_\infty$
0.2	2	$3.3863e - 04$		$4.7890e - 04$	
	2^2	$9.5675e - 05$	1.8235	$1.3530e - 04$	1.8235
	2^3	$2.6054e - 05$	1.8766	$3.6846e - 05$	1.8766
	2^4	$6.6519e - 06$	1.9697	$9.4072e - 06$	1.9697
	2^5	$1.4992e - 06$	2.1496	$2.1201e - 06$	2.1496
	2^6	$3.3167e - 07$	2.1763	$4.6905e - 07$	2.1763
0.3	2	$7.4798e - 04$		$1.0578e - 03$	
	2^2	$2.0921e - 04$	1.8380	$2.9587e - 04$	1.8380
	2^3	$5.6681e - 05$	1.8840	$8.0158e - 05$	1.8840
	2^4	$1.4749e - 05$	1.9423	$2.0858e - 05$	1.9423
	2^5	$3.4670e - 06$	2.0888	$4.9031e - 06$	2.0888
	2^6	$7.3543e - 07$	2.2370	$1.0401e - 06$	2.2370
0.5	2	$2.2598e - 03$		$3.1958e - 03$	
	2^2	$6.2388e - 04$	1.8568	$8.8230e - 04$	1.8568
	2^3	$1.6658e - 04$	1.9050	$2.3558e - 04$	1.9050
	2^4	$4.3188e - 05$	1.9475	$6.1078e - 05$	1.9475
	2^5	$1.0743e - 05$	2.0073	$1.5193e - 05$	2.0073
	2^6	$2.3470e - 06$	2.1945	$3.3192e - 06$	2.1945



TABLE 4. Errors \mathcal{L}_2 , \mathcal{L}_∞ and corresponding experimental order of convergences ${}_y EOC_2$, ${}_y EOC_{L_\infty}$ with $N = 500$, $\rho = 1.52$ for Example 5.2.

μ	M	\mathcal{L}_2 - error	${}_y EOC_2$	\mathcal{L}_∞ - error	${}_y EOC_\infty$
0.2	2	$7.4268e - 03$		$1.0503e - 02$	
	2^2	$1.9676e - 03$	1.9163	$2.6920e - 03$	1.9641
	2^3	$4.9603e - 04$	1.9880	$6.7724e - 04$	1.9909
	2^4	$1.2422e - 04$	1.9976	$1.6957e - 04$	1.9978
	2^5	$3.1065e - 05$	1.9995	$4.2408e - 05$	1.9995
	2^6	$7.7652e - 06$	2.0002	$1.0600e - 05$	2.0002
0.3	2	$7.4021e - 03$		$1.0468e - 02$	
	2^2	$1.9600e - 03$	1.9171	$2.6812e - 03$	1.9650
	2^3	$4.9402e - 04$	1.9882	$6.7441e - 04$	1.9912
	2^4	$1.2371e - 04$	1.9976	$1.6886e - 04$	1.9978
	2^5	$3.0935e - 05$	1.9996	$4.2225e - 05$	1.9996
	2^6	$7.7309e - 06$	2.0005	$1.0552e - 05$	2.0006
0.5	2	$7.3191e - 03$		$1.0351e - 02$	
	2^2	$1.9343e - 03$	1.9198	$2.6450e - 03$	1.9684
	2^3	$4.8727e - 04$	1.9890	$6.6490e - 04$	1.9921
	2^4	$1.2199e - 04$	1.9979	$1.6644e - 04$	1.9981
	2^5	$3.0500e - 05$	1.9999	$4.1611e - 05$	2.0000
	2^6	$7.6161e - 06$	2.0017	$1.0390e - 05$	2.0017

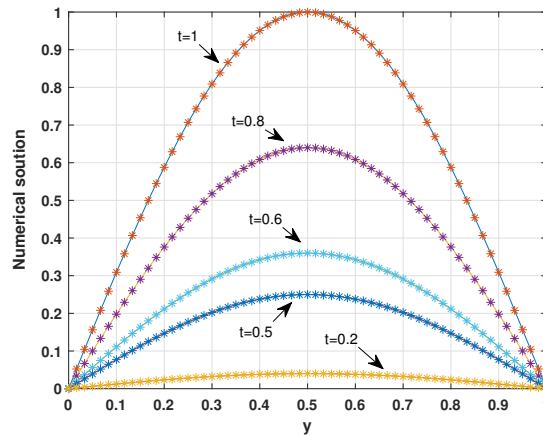


FIGURE 2. Numerical solution (starred line) and exact solution (solid line) of Example 5.1 with $\mu = 0.2$, $\rho = 0.1$ and $M = N = 60$ for different t .

Example 5.1. Consider the following test problem

$$\begin{cases} {}_0^{ABC} \mathcal{D}_t^\mu v(y, t) = v_{yy}(y, t) + F(y, t), & (y, t) \in \Omega := [0, 1] \times [0, 1], \\ v(y, 0) = 0, & 0 \leq y \leq 1, \\ v(0, t) = 0, v(1, t) = 0, & 0 \leq t \leq 1, \end{cases}$$



TABLE 5. Errors \mathcal{L}_2 , \mathcal{L}_∞ and corresponding experimental order of convergences tEOC_2 , ${}^tEOC_\infty$ with $M = 500$, $\rho = 1$ for Example 5.2.

μ	N	\mathcal{L}_2 - error	tEOC_2	\mathcal{L}_∞ - error	${}^tEOC_\infty$
0.2	2	$8.7467e - 05$		$1.2318e - 04$	
	2^2	$2.4780e - 05$	1.8196	$3.4900e - 05$	1.8195
	2^3	$6.8168e - 06$	1.8620	$9.6023e - 06$	1.8618
	2^4	$1.8108e - 06$	1.9124	$2.5525e - 06$	1.9115
	2^5	$4.4429e - 07$	2.0271	$6.2801e - 07$	2.0230
	2^6	$9.8670e - 08$	2.1708	$1.3953e - 07$	2.1702
0.3	2	$1.9308e - 04$		$2.7192e - 04$	
	2^2	$5.4074e - 05$	1.8362	$7.6153e - 05$	1.8362
	2^3	$1.4719e - 05$	1.8773	$2.0730e - 05$	1.8772
	2^4	$3.8995e - 06$	1.9163	$5.4939e - 06$	1.9158
	2^5	$9.8825e - 07$	1.9803	$1.3941e - 06$	1.9786
	2^6	$2.2187e - 07$	2.1551	$3.1389e - 07$	2.1509
0.5	2	$5.8315e - 04$		$8.2124e - 04$	
	2^2	$1.6106e - 04$	1.8562	$2.2682e - 04$	1.8562
	2^3	$4.3073e - 05$	1.9028	$6.0662e - 05$	1.9027
	2^4	$1.1236e - 05$	1.9387	$1.5826e - 05$	1.9385
	2^5	$2.8646e - 06$	1.9717	$4.0366e - 06$	1.9711
	2^6	$6.9088e - 07$	2.0518	$9.7529e - 07$	2.0492

with the source term

$$F(y, t) = \frac{2t^2}{(1 - \mu)} \sin(\pi y) E_{\mu,3} \left[\frac{-\mu}{1 - \mu} t^\mu \right] + \pi^2 t^2 \sin(\pi y),$$

and $B(\mu) = 1$. $v(y, t) = t^2 \sin(\pi y)$ is the analytical solution of this test problem.

Example 5.2. Consider the following test problem

$$\begin{cases} {}_0^{ABC} \mathcal{D}_t^\mu v(y, t) = v_{yy}(y, t) + F(y, t), & (y, t) \in \Omega := [0, 1] \times [0, 1], \\ v(y, 0) = 0, & 0 \leq y \leq 1, \\ v(0, t) = 0, v(1, t) = 0, & 0 \leq t \leq 1, \end{cases}$$

with the source term

$$F(y, t) = \frac{2}{(1 - \mu)} y(y - 1) t^2 E_{\mu,3} \left[\frac{-\mu}{1 - \mu} t^\mu \right] - 2t^2,$$

and $B(\mu) = 1$. $v(y, t) = y(y - 1) t^2$ is the analytical solution of this test problem.

Example 5.3. Consider the following test problem

$$\begin{cases} {}_0^{ABC} \mathcal{D}_t^\mu v(y, t) = v_{yy}(y, t) + F(y, t), & (y, t) \in \Omega := [0, 1] \times [0, 1], \\ v(y, 0) = 0, & 0 \leq y \leq 1, \\ v(0, t) = t^3, v(1, t) = et^3, & 0 \leq t \leq 1, \end{cases}$$

with the source term

$$F(y, t) = \frac{6}{(1 - \mu)} e^y t^3 E_{\mu,4} \left[\frac{-\mu}{1 - \mu} t^\mu \right] - t^3 e^y,$$



TABLE 6. Errors \mathcal{L}_2 , \mathcal{L}_∞ and corresponding experimental order of convergences ${}_yEOC_2$, ${}_yEOC_\infty$ with $N = 512$, $\rho = 1.52$ for Example 5.3.

μ	M	\mathcal{L}_2 - error	${}_yEOC_2$	\mathcal{L}_∞ - error	${}_yEOC_\infty$
0.2	2	$3.5858e-03$		$5.0710e-03$	
	2^2	$9.4592e-04$	1.9225	$1.2875e-03$	1.9776
	2^3	$2.3802e-04$	1.9906	$3.2319e-04$	1.9942
	2^4	$5.9610e-05$	1.9975	$8.1489e-05$	1.9877
	2^5	$1.4942e-05$	1.9961	$2.0435e-05$	1.9956
	2^6	$3.7720e-06$	1.9860	$5.1624e-06$	1.9849
0.3	2	$3.5703e-03$		$5.0491e-03$	
	2^2	$9.4120e-04$	1.9235	$1.2809e-03$	1.9789
	2^3	$2.3682e-04$	1.9907	$3.2149e-04$	1.9943
	2^4	$5.9338e-05$	1.9968	$8.1109e-05$	1.9868
	2^5	$1.4907e-05$	1.9929	$2.0383e-05$	1.9925
	2^6	$3.7962e-06$	1.9734	$5.1949e-06$	1.9722
0.5	2	$3.5174e-03$		$4.9743e-03$	
	2^2	$9.2510e-04$	1.9268	$1.2582e-03$	1.9832
	2^3	$2.3270e-04$	1.9911	$3.1568e-04$	1.9948
	2^4	$5.8399e-05$	1.9945	$7.9798e-05$	1.9840
	2^5	$1.4774e-05$	1.9829	$2.0190e-05$	1.9827
	2^6	$3.8653e-06$	1.9344	$5.2872e-06$	1.9331

TABLE 7. Comparison with method in [39] taking $N = 500$ for Example 5.3.

α	M	Present method		Method in [39]	
		\mathcal{L}_∞ - error	${}_xO_{\mathcal{L}_\infty}$	\mathcal{L}_∞ - error	${}_xO_{\mathcal{L}_\infty}$
0.2	20	2.9807e-05	-	1.5816e-04	-
	40	7.3984e-06	2.0104	3.9767e-05	1.9917
	80	1.7977e-06	2.0410	9.8876e-06	2.0079
	160	3.9766e-07	2.1766	2.4200e-06	2.0306
	320	4.7599e-08	3.0625	5.5323e-07	2.1290
0.3	20	2.9581e-05	-	1.5723e-04	-
	40	7.2945e-06	2.0198	3.9488e-05	1.9934
	80	1.7243e-06	2.0808	9.7702e-06	2.0149
	160	3.3190e-07	2.3775	2.3432e-06	2.0599
	320	4.5079e-08	2.8802	4.8662e-07	2.2676

TABLE 8. Errors \mathcal{L}_2 , \mathcal{L}_∞ and corresponding experimental order of convergences tEOC_2 , ${}^tEOC_\infty$ with $M = 500$, $\rho = 1.52$ for Example 5.3.

μ	N	\mathcal{L}_2 - error	tEOC_2	\mathcal{L}_∞ - error	${}^tEOC_\infty$
0.2	2	$1.4382e - 03$		$1.9684e - 03$	
	2^2	$4.4507e - 04$	1.6921	$6.0916e - 04$	1.6921
	2^3	$1.2927e - 04$	1.7837	$1.7693e - 04$	1.7837
	2^4	$3.6218e - 05$	1.8356	$4.9572e - 05$	1.8355
	2^5	$9.9400e - 06$	1.8654	$1.3605e - 05$	1.8654
	2^6	$2.7149e - 06$	1.8724	$3.7159e - 06$	1.8724
0.3	2	$3.1403e - 03$		$4.2979e - 03$	
	2^2	$9.5553e - 04$	1.7165	$1.3077e - 03$	1.7165
	2^3	$2.7270e - 04$	1.8090	$3.7322e - 04$	1.8090
	2^4	$7.5035e - 05$	1.8617	$1.0269e - 04$	1.8617
	2^5	$2.0195e - 05$	1.8936	$2.7639e - 05$	1.8936
	2^6	$5.3795e - 06$	1.9084	$7.3625e - 06$	1.9084
0.5	2	$9.4297e - 03$		$1.2902e - 02$	
	2^2	$2.8082e - 03$	1.7476	$3.8423e - 03$	1.7476
	2^3	$7.7972e - 04$	1.8486	$1.0669e - 03$	1.8486
	2^4	$2.0838e - 04$	1.9038	$2.8512e - 04$	1.9037
	2^5	$5.4473e - 05$	1.9356	$7.4534e - 05$	1.9356
	2^6	$1.4071e - 05$	1.9528	$1.9253e - 05$	1.9528

and $B(\mu) = 1$. $v(y, t) = t^3 e^y$ is the analytical solution of this test problem.

Tables 1, 4, and 6 display \mathcal{L}_2 - error, \mathcal{L}_∞ - error, and corresponding spatial orders of convergence yEOC_2 and ${}^yEOC_\infty$ for Examples 5.1, 5.2, and 5.3, respectively for different choices of the fractional order μ . From these tables, we see that the errors are decreasing as the mesh size decreases, and that the estimated spatial order of convergence is two. This is in agreement with the theoretical order of convergence obtained in Theorem 4.2.2. Similarly, the \mathcal{L}_2 - error, \mathcal{L}_∞ - error, and corresponding orders of convergence tEOC_2 and ${}^tEOC_\infty$ in the temporal direction for Examples 5.1, 5.2, and 5.3 have been calculated using the formulae (5.2), (5.1), and (5.3) and are shown in Tables 3, 5, and 8, respectively for different choices of the fractional order μ . These tables show a second-order convergence in time, which is in agreement with Theorem 4.2.2.

Moreover, Table 2 highlights the comparison between our proposed scheme and central difference scheme as outlined in [49]. The results indicate that the spatial convergence order of the proposed scheme is 2, aligning with the findings in [49]. Importantly, our work has elevated the accuracy order beyond that of the referenced scheme. In a similar manner, Table 7 presents a comparison between our proposed scheme and the cubic B-spline collocation method outlined in [39]. The results highlight a spatial convergence order of 2 for our scheme, consistent with the results reported in [39]. Importantly, our work has surpassed the accuracy order achieved by the referenced method.

In Figures 1, 3 and 5, 3-d plots of the numerical solutions of Examples 5.1, 5.2, and 5.3 are shown, respectively with $M = N = 60$ and for different fractional orders μ . Figure 2 compares the numerical solution and the exact solution of Example 5.1, with $\mu = 0.2$, $\rho = 0.1$ and $M = N = 60$ at different time levels. From this graph we can observe that the numerical solution runs concurrently with the exact solution. In a similar manner Figures 4 and 6 compare the numerical solution and the exact solution of Examples 5.2 and 5.3 respectively for a different choice of μ , ρ , M and N . From these graphs it is evident that the numerical solutions match well with the exact solutions. In summary, the numerical results presented in this section are in good agreement with our theoretical findings.



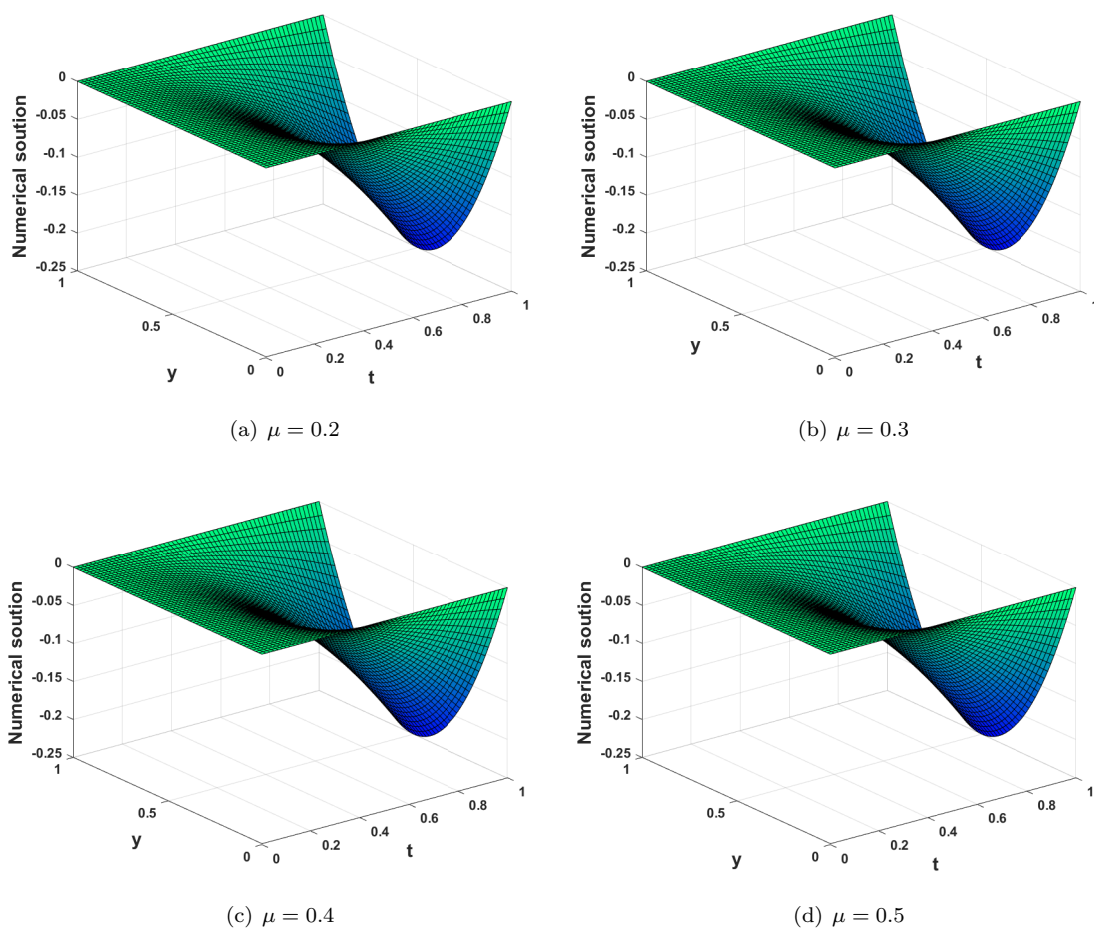


FIGURE 3. Numerical solution of Example 5.2 with $M = N = 60$ and $\rho = 1.52$.

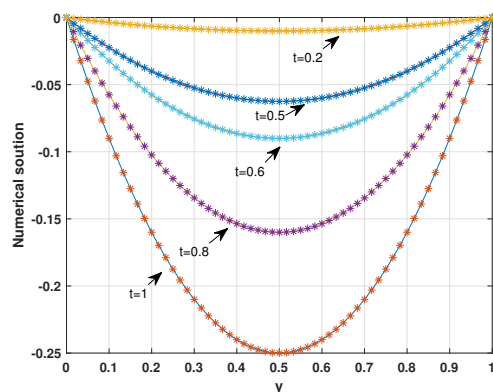


FIGURE 4. Numerical solution (starred line) and exact solution (solid line) of Example 5.2 with $\mu = 0.5$, $\rho = 1$ and $M = N = 60$ for different t .

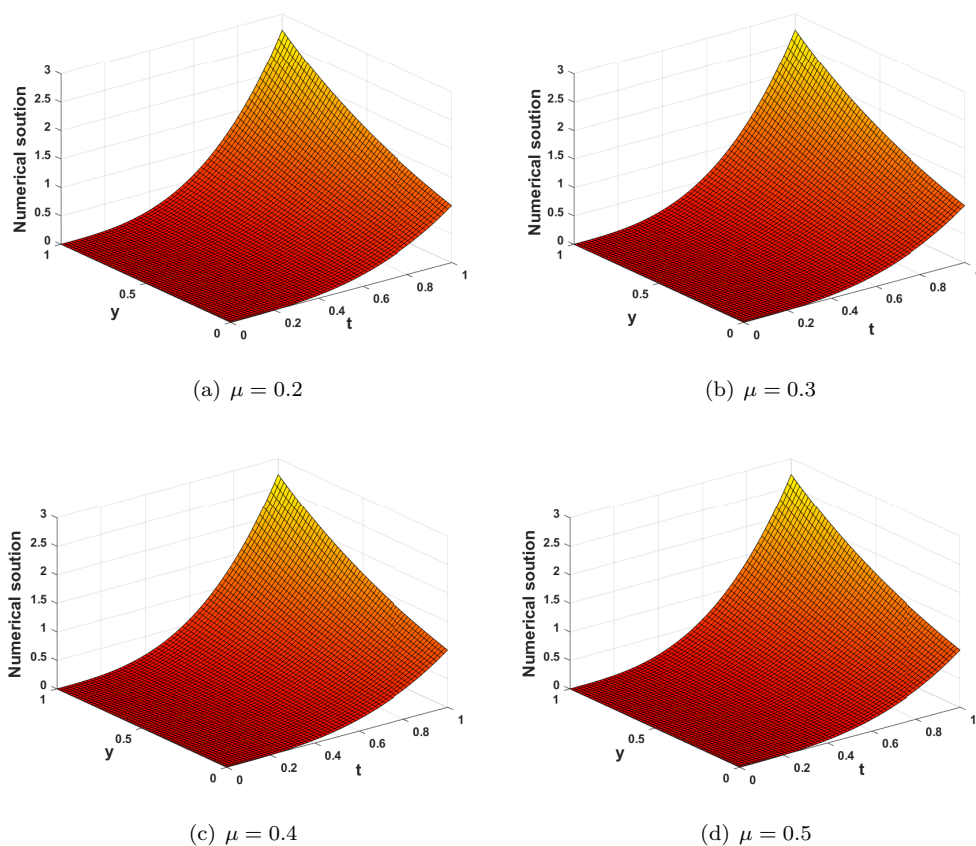


FIGURE 5. Numerical solution of Example 5.3 with $M = N = 60$ and $\rho = 1$.

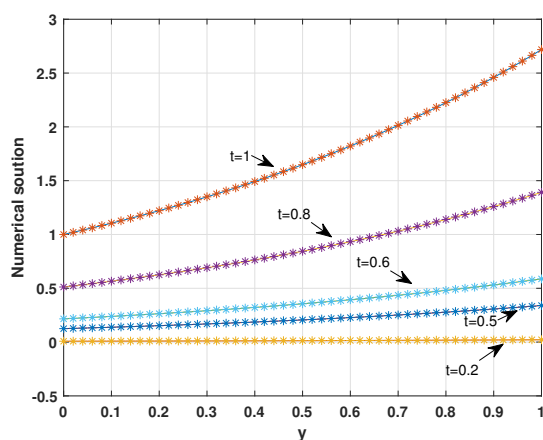


FIGURE 6. Numerical solution (starred line) and exact solution (solid line) of Example 5.3 with $\mu = 0.5$, $\rho = 1$ and $M = N = 50$ for different t .

6. CONCLUSION

For the time-fractional sub-diffusion equation with ABC time fractional operator of order $0 < \mu \leq \frac{1}{2}$, an efficient and convenient collocation method is introduced in the proposed work. A finite difference method is employed to discretize the ABC fractional operator and exponential B-spline functions are used for spatial discretization. The unconditional stability of the method has been proven through the von Neumann method. In addition, the proposed method has been shown to provide a unique solution. The convergence analysis of the proposed method has been proved rigorously and it is shown that the order of convergence is $O(h_t^2, h_y^2)$. Finally, the current scheme has been implemented on three test problems, thus confirming the theoretical results and showing the viability of the proposed scheme. Our goal for the future is to broaden the scope of our current approach, addressing not only linear fractional problems but also solving non-linear fractional problems and time-fractional problems in higher dimensions.

Acknowledgements: The authors would like to express great appreciation to the anonymous reviewers for their valuable comments and constructive suggestions, which have helped to improve the quality and presentation of this paper.

Conflict of Interest: The authors have no relevant financial or non-financial interests to disclose.

Funding: The authors did not receive support from any organization for the submitted work.

Data availability: No data was used for the research described in the article.

REFERENCES

- [1] M. N. Alam, H. S. Akash, U. Saha, M. S. Hasan, M. W. Parvin, and C. Tun, *Bifurcation Analysis and Solitary Wave Analysis of the Nonlinear Fractional Soliton Neuron Model*, Iranian Journal of Science, 47 (2023), 1797–1808.
- [2] M. N. Alam and S. M. R. Islam, *The agreement between novel exact and numerical solutions of nonlinear models*, Partial Differential Equations in Applied Mathematics, 8 (2023), 100584.
- [3] T. Allahviranloo and B. Ghanbari, *On the fuzzy fractional differential equation with interval Atangana-Baleanu fractional derivative approach*, Chaos, Solitons & Fractals, 130 (2020), 109397.
- [4] F. Amblard, A. C. Maggs, B. Yurke, A. N. Pargellis, and S. Leibler, *Subdiffusion and anomalous local viscoelasticity in actin networks*, Physical review letters, 77 (1996), 4470.
- [5] I. Ardelean, G. Farrhera, and R. Kimmich, *Effective diffusion in partially filled nanoscopic and microscopic pores*, Journal of Optoelectronics and Advanced Materials, 9 (2007), 655.
- [6] A. Atangana and D. Baleanu, *New fractional derivatives with nonlocal and non-singular kernel: theory and application to heat transfer model*, arXiv preprint arXiv:1602.03408, (2016).
- [7] E. Barkai, *CTRW pathways to the fractional diffusion equation*, Chemical Physics, 284 (2002), 13–27.
- [8] C. D. Boor, *A practical guide to splines*, 27 (1978).
- [9] M. Caputo and M. Fabrizio, *A new definition of fractional derivative without singular kernel*, Progr. Fract. Differ. Appl, 1 (2015), 73–85.
- [10] Y. Cicek, N. G. Kaymak, E. Bahar, G. Gurarslan, and G. Tangolu, *A new numerical algorithm based on Quintic B-Spline and adaptive time integrator for Coupled Burgers equation*, Computational Methods for Differential Equations, 11 (2023), 130–142.
- [11] C. M. Chen, F. Liu, I. Turner, and V. Anh, *A Fourier method for the fractional diffusion equation describing sub-diffusion*, Journal of Computational Physics, 227 (2007), 886–897.
- [12] A. Dokoumetzidis and P. Macheras, *Fractional kinetics in drug absorption and disposition processes*, Journal of pharmacokinetics and pharmacodynamics, 36 (2009), 165–178.
- [13] R. Ghaffari and F. Ghoreishi, *Reduced spline method based on a proper orthogonal decomposition technique for fractional sub-diffusion equations*, Applied Numerical Mathematics, 137 (2019), 62–79.



- [14] B. Ghanbari and D. Kumar, *Numerical solution of predator-prey model with Beddington-DeAngelis functional response and fractional derivatives with Mittag-Leffler kernel*, *Chaos: An Interdisciplinary Journal of Nonlinear Science*, *29* (2019), 63–103.
- [15] R. Gorenflo and F. Mainardi, *Random walk models approximating symmetric space-fractional diffusion processes*, *Problems and methods in mathematical physics*, (2001), 120–145.
- [16] Y. Gu and P. Zhuang, *Anomalous sub-diffusion equations by the meshless collocation method*, *Australian Journal of Mechanical Engineering*, *10* (2012), 1–8.
- [17] V. Gupta and M. K. Kadalbajoo, *Qualitative analysis and numerical solution of burgers equation via B-spline collocation with implicit euler method on piecewise uniform mesh*, *Journal of Numerical Mathematics*, *24* (2016), 73–94.
- [18] M. Heydari, *Wavelets Galerkin method for the fractional subdiffusion equation*, *Journal of Computational and Nonlinear Dynamics*, *11* (2016), 061014.
- [19] J. Hristov, *Approximate solutions to fractional subdiffusion equations*, *The European Physical Journal Special Topics*, *193* (2011), 229–243.
- [20] M. K. Kadalbajoo, V. Gupta, and A. Awasthi, *A uniformly convergent B-spline collocation method on a nonuniform mesh for singularly perturbed one-dimensional time-dependent linear convection-diffusion problem*, *Journal of Computational and Applied Mathematics*, *220* (2008), 271–289.
- [21] M. K. Kadalbajoo and V. Gupta, *Numerical solution of singularly perturbed convection-diffusion problem using parameter uniform B-spline collocation method*, *Journal of Mathematical Analysis and Applications*, *355* (2009), 439–452.
- [22] M. K. Kadalbajoo and V. Gupta, *A parameter uniform B-spline collocation method for solving singularly perturbed turning point problem having twin boundary layers*, *International Journal of Computer Mathematics*, *87* (2010), 3218–3235.
- [23] A. Kanth and N. Garg, *A numerical approach for a class of time-fractional reaction-diffusion equation through exponential B-spline method*, *Computational and Applied Mathematics*, *39* (2020), 1–24.
- [24] B. Karaagac, K. M. Owolabi, and K. S. Nisar, *Analysis and dynamics of illicit drug use described by fractional derivative with Mittag-Leffler kernel*, *CMC-Comput Mater Cont*, *65*(3) (2020), 1905–1924.
- [25] M. Karta, *A new application for numerical computations of the modified equal width equation (MEW) based on Lumped Galerkin method with the cubic B-spline*, *Computational Methods for Differential Equations*, *11* (2023), 95–107.
- [26] S. Kumar, V. Gupta, and J. Gómez-Aguilar, *An efficient operational matrix technique to solve the fractional order non-local boundary value problems*, *Journal of Mathematical Chemistry*, *60* (2022), 1463–1479.
- [27] T. Langlands and B. I. Henry, *The accuracy and stability of an implicit solution method for the fractional diffusion equation*, *Journal of Computational Physics*, *205* (2005), 719–736.
- [28] W. H. Luo, T. Z. Huang, G. C. Wu, and X. M. Gu, *Quadratic spline collocation method for the time fractional subdiffusion equation*, *Applied Mathematics and Computation*, *276* (2016), 252–265.
- [29] F. Mainardi, *Fractional diffusive waves in viscoelastic solids*, *Nonlinear waves in solids*, *137* (1995), 93–97.
- [30] B. J. McCartin, *Theory of exponential splines*, *Journal of Approximation Theory*, *66* (1991), 1–23.
- [31] J. D. Moisset, L. Carrier, and P. A. Johnson, *Perturbative corrections for Hartree-Fock-like algebraic Bethe ansatz analogue*, *Journal of Mathematical Chemistry*, *60* 2022, 1707–1724.
- [32] I. Podlubny, *Fractional differential equations: an introduction to fractional derivatives, fractional differential equations, to methods of their solution and some of their applications*, Elsevier, 1998.
- [33] D. Prakasha, P. Veerasha, and H. M. Baskonus, *Analysis of the dynamics of hepatitis E virus using the Atangana-Baleanu fractional derivative*, *The European Physical Journal Plus*, *134* (2019), 1–11.
- [34] S. Pruess, *Properties of splines in tension*, *Journal of Approximation Theory*, *17* (1976), 86–96.
- [35] S. Pruess, *Alternatives to the exponential spline in tension*, *Mathematics of Computation*, *33* (1979), 1273–1281.
- [36] S. C. S. Rao and M. Kumar, *Exponential B-spline collocation method for self-adjoint singularly perturbed boundary value problems*, *Applied Numerical Mathematics*, *58* (2008), 1572–1581.
- [37] P. Roul and VMK. P. Goura, *A high-order B-spline collocation scheme for solving a nonhomogeneous time-fractional diffusion equation*, *Mathematical Methods in the Applied Sciences*, *44* (2021), 546–567.
- [38] P. Roul, *A robust numerical technique and its analysis for computing the price of an Asian option*, *Journal of Computational and Applied Mathematics*, *416* (2022), 114527.

- [39] M. Shafiq, M. Abbas, K. M. Abualnaja, M. J. Huntul, A. Majeed, and T. Nazir, *An efficient technique based on cubic B-spline functions for solving time-fractional advection diffusion equation involving Atangana–Baleanu derivative*, *Engineering with Computers*, *38* (2022), 901–917.
- [40] A. Singh, S. Kumar, and J. Vigo-Aguiar, *On new approximations of Caputo–Prabhakar fractional derivative and their application to reaction–diffusion problems with variable coefficients*, *Mathematical Methods in the Applied Sciences*, *47* (2023), 268–296.
- [41] A. Singh, S. Kumar, and J. Vigo-Aguiar, *A fully discrete scheme based on cubic splines and its analysis for time-fractional reaction–diffusion equations exhibiting weak initial singularity*, *Journal of Computational and Applied Mathematics*, *434* (2023), 115338.
- [42] A. Singh and S. Kumar, *An Efficient Numerical Method Based on Exponential B-splines for a Time-Fractional Black–Scholes Equation Governing European Options*, *Computational Economics*, (2023), 1–38.
- [43] A. Singh and S. Kumar, *A convergent exponential B-spline collocation method for a time-fractional telegraph equation*, *Computational and Applied Mathematics*, *42* (2023), 79.
- [44] A. Singh, S. Kumar, and J. Vigo-Aguiar, *High-order schemes and their error analysis for generalized variable coefficients fractional reaction–diffusion equations*, *Mathematical Methods in the Applied Sciences*, *46* (2023), 16521–16541.
- [45] S. Singh and D. Kumar, *Spline-based parameter-uniform scheme for fourth-order singularly perturbed differential equations*, *Journal of Mathematical Chemistry*, *60* (2022), 1872–1902.
- [46] S. T. Thabet, M. S. Abdo, K. Shah, and T. Abdeljawad, *Study of transmission dynamics of COVID-19 mathematical model under ABC fractional order derivative*, *Results in Physics*, *18* (2020), 103507.
- [47] J. M. Varah, *A lower bound for the smallest singular value of a matrix*, *Linear Algebra and its applications*, *11* (1975), 3–5.
- [48] S. Yadav and R. K. Pandey, *Numerical approximation of fractional Burgers’ equation with Atangana–Baleanu derivative in Caputo sense*, *Chaos, Solitons & Fractals*, *133* (2020), 109630.
- [49] S. Yadav and R. K. Pandey, *Numerical approximations of Atangana–Baleanu–Caputo derivative and its application*, *Chaos, Solitons & Fractals*, *118* (2019), 58–64.
- [50] S. B. Yuste and L. Acedo, *An explicit finite difference method and a new von Neumann-type stability analysis for fractional diffusion equations*, *SIAM Journal on Numerical Analysis*, *42* (2005), 1862–1874.
- [51] S. B. Yuste, *Weighted average finite difference methods for fractional diffusion equations*, *Journal of Computational Physics*, *216* (2006), 264–274.

